

## SENSITIVITY OF A NEW VELOCITY/PRESSURE-GRADIENT MODEL TO THE REYNOLDS NUMBER

Svetlana V. Poroseva

Department of Mechanical Engineering  
University of New Mexico  
Albuquerque, New Mexico, 87131-0001, U.S.A.  
poroseva@unm.edu

Scott M. Murman

NASA Ames Research Center  
Mountain View, California, 94035, U.S.A.  
Scott.M.Murman@nasa.gov

### ABSTRACT

The paper presents results of validation of a new model for velocity/pressure-gradient correlations in planar wall-bounded incompressible turbulent flows. The model belongs to a class of data-driven models and was obtained from the analysis of direct numerical simulation (DNS) data collected in a fully developed channel flow at  $Re_\tau = 392$ . It includes only the terms originally present in the transport equations for the Reynolds stresses. In the paper, sensitivity of the model coefficients to the flow Reynolds number and geometry is tested using three other DNS databases, with the Reynolds numbers,  $Re_\tau$  and  $Re_\theta$ , varying from 392 to 5200 in a fully developed channel flow and from 300 to 6500 in a zero-pressure-gradient boundary-layer over a flat plate, respectively. In addition, the model is validated using DNS data in a strained channel flow at eight strain times including those that cause the flow to separate. It is demonstrated that no tuning of the model coefficients is required to accurately reproduce the behaviour of velocity/pressure-gradient correlations right to the wall in all considered flows.

### INTRODUCTION

When simulating turbulent flows with the Reynolds-averaged Navier-Stokes (RANS) equations, models for unknown terms in the equations are required. Among such terms are velocity/pressure-gradient (VPG) correlations.

Traditional approach to modelling the VPG correlations can be traced back to Chou (1945) and is based on the analysis of the exact integro-differential expressions for the VPG correlations. In the approach, the goal is to preserve tensor properties of the two-point turbulence statistics that are integrated over the entire flow domain in models for one-point VPG correlations. Various linear and non-linear models were developed in such a manner over the years (see, e.g., Hanjalić and Launder, 2011). However, as demonstrated by many studies, values of model coefficients have to vary in any of these models. Ad-hoc or empirical corrections have to be implemented into a model to describe the turbulent flow features in different flow geometries and at different Reynolds numbers, also near a wall, under rotation etc. A presence of the flow separation reduces predictive capability of such models as well.

In Poroseva and Murman (2014a), we analysed the major assumptions used in the traditional approach to modelling one-point VPG correlations, proposed new models for the VPG correlations up to the fourth order, which are free of the

homogeneous flow assumption, and analysed predictive capabilities of the derived models in *a priori* testing with DNS data in planar wall-bounded flows (Spalart, 1988; Sillero et al., 2013; Jeyapaul et al., 2015). The study led us to conclude that the traditional approach is unlikely to result in models for VPG correlations that are accurate near a wall.

A more promising approach to modelling VPG correlations in wall-bounded flows was proposed in Poroseva and Murman (2014a,b). In the approach, model expressions for VPG correlations up to the fourth order were obtained from the direct analysis of DNS data in a fully developed channel flow at  $Re_\tau = 392$  based on the friction velocity and the channel half-width (Jeyapaul et al., 2015). When these new model expressions for the second-order VPG correlations were tested using DNS data in a zero-pressure gradient boundary layer (ZPGBL) over a flat plate at different Reynolds numbers (Spalart, 1988; Sillero et al., 2013), the results of the same level of accuracy as in the channel flow were obtained without changing the model coefficients (Poroseva and Murman, 2014a). Due to the lack of DNS data for the budget terms in transport equations for higher-order velocity moments, the model expressions for higher-order VPG correlations could not be tested when the study was conducted.

Motivated by success of the initial models, a new set of data-driven models for VPG correlations in the transport equations for the Reynolds stresses  $\langle u^2 \rangle$ ,  $\langle v^2 \rangle$ , and  $\langle uv \rangle$  were proposed in Poroseva et al. (2015), with the models performance being improved in the flow area at  $y_+ < 10$ , that is, in immediate vicinity to a wall. Here,  $y_+ = yu_\tau / \nu$  is the normal-to-wall coordinate  $y$  in the wall units;  $u_\tau$  and  $\nu$  are the friction velocity and the kinematic viscosity, respectively;  $u$  and  $v$  are velocity fluctuations in streamwise and normal-to-wall directions. The new models were also obtained from the analysis of DNS data in a fully developed channel flow at  $Re_\tau = 392$  (Jeyapaul et al., 2015). The current paper presents results of validation of these models using different DNS datasets in a fully-developed channel flow and in a ZPGBL at various Reynolds numbers. Also, predictive capability of the models in a separated flow is evaluated.

### VELOCITY/PRESSURE-GRADIENT CORRELATION MODELS

The models for VPG correlations proposed in Poroseva et al. (2015) and tested in the current study are:

$$\Pi_{xy} = -0.92D_{xy}^T - 0.92P_{xy} - 0.3D_{xy}^M$$

$$\Pi_{xx} = -0.78\Pi_{xy} - 0.7\Pi_{yy} - 0.25D_{xy}^T + 0.01D_{xx}^M \quad (1)$$

$$\begin{aligned} \Pi_{yy} = & -0.45P_{xy} - 0.031P_{xx} - 1.35D_{yy}^T + 1.15D_{zz}^T \\ & - 0.47D_{xy}^T + 0.2D_{yy}^M \end{aligned}$$

Here,  $\Pi_{ij} = -1/\rho(\langle u_i \partial p / \partial x_j \rangle + \langle u_j \partial p / \partial x_i \rangle)$  are the VPG correlations in the Reynolds stress transport equations. The other terms in (1) are standard budget terms in the Reynolds stress transport equations: production,  $P_{ij}$ , turbulent diffusion,  $D_{ij}^T$ , and molecular diffusion,  $D_{ij}^M$ . Indices  $x$  and  $y$  indicate streamwise and normal-to-wall flow directions, respectively. Notice that expressions (1) include only existing terms in the Reynolds stress transport equations.

In the form provided, models (1) are suitable for planar wall-bounded flows only, where the positive direction of  $y$  is from the wall, with  $y = 0$  at the wall. DNS data in free-shear and three-dimensional turbulent flows have to be analyzed as well to complete a tensor-invariant model for the correlations. The accuracy of DNS data used in the analysis has also to be improved with respect to the ratio of balance errors to molecular and turbulent diffusion terms in the DNS budgets of all considered datasets (Poroseva et al., 2016a,b). The DNS data accuracy is the main reason why the model for  $\Pi_{zz}$  is currently excluded from consideration.

## DNS DATASETS

In the current study, model expressions (1) are tested in a fully developed channel flow using the DNS data from Lee and Moser (2015) at three Reynolds numbers  $Re_\tau$ : 550, 1000, and 5200. Data in a ZPGBL from two DNS databases (Spalart, 1988, Sillero et al., 2013) are also used. The data from Spalart (1988) are at three Reynolds numbers  $Re_\theta$  based on the momentum thickness: 300, 670, and 1410. The data from Sillero et al. (2013) are at six  $Re_\theta$  in a range from 4000 to 6500 with an increment of 500. The models are also validated in a planar strained turbulent channel flow with the DNS data from Coleman et al. (2013) collected at  $Re_\tau = 392$ . The strained channel flow is of interest for the models validation because it reproduces the main features of a spatially developing adverse-pressure gradient boundary layer over a flat plate. This is achieved by simultaneously applying streamwise in-plane channel wall motion and straining the entire flow domain of an initially fully developed turbulent channel flow. The channel walls decelerate in the streamwise direction and diverge in the normal-to-wall direction. At certain conditions, the flow separates from the wall. The parameter used to characterize the flow conditions is  $A_{22}t$ , where  $A_{22} = \partial V / \partial y$  is the normal-to-wall flow divergence,  $V$  is the mean flow velocity component in the normal-to-wall direction, and  $t$  is time during which the initial flow domain deformation is applied. The flow

reverses at  $A_{22}t = 0.675$ . In our study, DNS data corresponding to eight values of  $A_{22}t$ : 0, 0.02, 0.1, 0.191, 0.281, 0.365, 0.675, and 0.772, are used to validate expressions (1). The unstrained channel flow data in Coleman et al. (2013) are the same as in Jeyapaul et al. (2015).

## RESULTS

This section presents results of *a priori* testing of model expressions (1). In the procedure, terms on the right-hand side of expressions (1) are substituted with the DNS data for the budget terms in the Reynolds stress transport equations. The VPG correlations calculated from (1) are compared then with DNS profiles for the terms on the left-hand side of (1). Values of the model coefficients in (1) remain unchanged in all calculations.

Figures 1 and 2 show the results of *a priori* testing of expressions (1) with DNS data from Lee and Moser (2015) in a fully developed channel flow and from Spalart (1988) in a ZPGBL, respectively. In these and following figures, all values are in wall units. Profiles of the VPG correlations calculated from (1) are shown by solid black lines and those from DNS by circles in the figures. Similar notations are adopted in Figs. 3 and 4.

Figure 3 compares the model profiles and those from DNS of the VPG correlations in a ZPGBL using the data from Sillero et al. (2013) at three Reynolds numbers  $Re_\theta$ : 4000, 5500, and 6500. The results obtained using the same dataset at the other three Reynolds numbers ( $Re_\theta = 4500, 5000, \text{ and } 6000$ ) (not shown here), are similar to those in Fig. 3.

Figures 4a-h demonstrate the models' performance in a strained channel flow with the data from Coleman et al. (2003) at all available strain times including the two times,  $A_{22}t = 0.675$  and 0.772, when the flow separates from the channel wall. (Figure 4i is the zoomed-in Fig. 4h.) Notice that with  $A_{22}t$  increasing, the three VPG correlations diminish in DNS. Models (1) correctly reproduce this behaviour of the VPG correlations.

Overall, the VPG correlations calculated from model expressions (1) are in a good agreement with their DNS profiles in the considered flow geometries at various Reynolds numbers, also at various strain times in the channel flow. That is, the proposed models correctly reflect physical processes associated with the VPG correlations.

In particular, they highlight a relation between the VPG correlations and molecular diffusion. Molecular diffusion is traditionally excluded from the VPG correlation models (Hanjalić & Launder, 2011). However, viscous processes are dominant near a wall at any Reynolds number. This is illustrated in Fig. 5 with the data from Lee & Moser (2015) as an example. (Production terms are not shown in Fig. 5 because they appear at the same location as turbulent diffusion terms and do not add to the discussion.) The DNS data shows that in the flow area where viscous diffusion and dissipation,  $\varepsilon_{ij}$ , prevail, the transport equations for Reynolds stresses can be reduced to

$$\Pi_{ij} + D_{ij}^M - \varepsilon_{ij} = 0 \quad (2)$$

with  $\Pi_{xx}$ ,  $\Pi_{yy}$ , and  $\Pi_{xy}$  being modelled as:

$$\Pi_{ij} = C \cdot D_{ij}^M \quad (3)$$

The coefficient  $C$  in (3) is of a constant value that varies for different  $\Pi_{ij}$  as seen in (1).

Figures 5 and 6 show the range of applicability of (2) for each of the three Reynolds stresses in different flows. In the figures, expression (2) with the added DNS budget balance errors,  $\Pi_{ij} + D_{ij}^M - \varepsilon_{ij} - Err_{ij}$ , is plotted to improve the figure quality. As the figures demonstrate, the applicability range of (2) is not affected by the Reynolds number or by the strain time. However, it varies from one Reynolds stress to another. The largest area,  $y_+ \leq 4$ , is for  $\langle v^2 \rangle$ , which is the Reynolds stress in the direction normal to a wall. The shortest is for  $\langle u^2 \rangle$ :  $y_+ \leq 0.5$ . For  $\langle uv \rangle$  and  $\langle w^2 \rangle$  (not shown here), the applicability range of (2) is at  $y_+ \leq 1$ . Even though the determined areas seem to be small, correct modelling of  $\Pi_{ij}$  in these areas proved to be of significance for the accurate modelling the VPG correlations outside these areas.

Another interesting feature of models (1) is that all of the models include the turbulent diffusion term  $D_{xy}^T$ . This is essential for the locations of extreme points in the model  $\Pi_{ij}$  - profiles matching those in the DNS profiles of corresponding VPG correlations. On the other hand, we also found that this particular term is responsible for a slight growth in the  $\Pi_{yy}$  -profile observed with the increase of the Reynolds number at  $y_+ = 6-8$  as seen in Figs. 1-3. Further investigation is required to clarify this issue.

Notice that no simple relation between  $\Pi_{xx}$  and the production terms was found from the data analysis. Instead, the analysis has revealed a relation between the three VPG correlations.

Because models (1) are obtained by analyzing DNS data, it is of importance to investigate how the data accuracy affects the models. As previously mentioned, models (1) were obtained from the analysis of data provided in Jeyapaul et al. (2015). The dataset from Lee & Moser (2015) is more accurate (Poroseva et al., 2016a). With these data, we found that the following model

$$\Pi_{xy} = -0.8D_{xy}^T - 0.95P_{xy} - 0.3D_{ij}^M \quad (4)$$

produces more accurate results for  $\Pi_{xy}$  in all considered flows as seen in Figs. 1-4. In the figures, model profiles obtained from (4) are shown by the red lines. Figures 2a and b are an exception that can be viewed as the Reynolds number effect, but the data used in Figs. 2a,b are also less accurate near a wall than those from other datasets at higher Re as seen in Fig. 7.

Notice, that the terms in model (4) are the same as in  $\Pi_{xy}$  - model (1). That is, the dataset accuracy affects the model coefficient values, not the model itself. Since uncertainty is present in any data (experimental, DNS, etc.) including those from Lee and Moser (2015), the data analysis can only provide approximate values for the model coefficients. RANS simulations with the VPG models will help to further verify the coefficient values.

## CONCLUSIONS

Our study demonstrated an excellent agreement between the DNS profiles for three VPG correlations:  $\Pi_{xx}$ ,  $\Pi_{yy}$ , and  $\Pi_{xy}$ , and the proposed models for these correlations in the considered planar wall-bounded turbulent flows in a wide range of Reynolds numbers and also in a presence of the flow separation. The agreement between the DNS and model profiles was obtained in all flow areas including the wall vicinity without variation of the model coefficients and without ad-hoc wall functions. In their current form, the proposed models are a proof of the concept that VPG correlations can be modelled as linear functions of only the existing terms in the Reynolds stress transport equations. This leaves as unknown only the turbulent diffusion and viscous dissipation terms in the RANS equations.

## REFERENCES

- Chou, P. Y., 1945, "On the velocity correlations and the solutions of the equations of turbulent fluctuation", *Q. J. Appl. Math.*, Vol. 3, pp. 38-54.
- Coleman, G. N., Kim, J., and Spalart, P. R., 2003, "Direct numerical simulation of a decelerated wall-bounded turbulent shear flow", *J. Fluid Mech.*, Vol. 495, pp. 1-18.
- Hanjalić, K. and Launder, B., 2011, *Modelling Turbulence in Engineering and the Environment*, Cambridge University Press, Cambridge, UK.
- Jeyapaul, E., Coleman, G. N., Rumsey, C. L., 2015, "Higher-order and length-scale statistics from DNS of a decelerated planar wall-bounded turbulent flow", *Int. J. Heat and Fluid Flow*, Vol. 54, pp. 14-27.
- Lee, M. and Moser, R. D., 2015, "Direct numerical simulation of turbulent channel flow up to  $Re_\tau = 5200$ ", *J. Fluid Mech.* Vol. 774, pp. 395-415.
- Poroseva, S. V., and Murman, S. M., 2014a, "Velocity/Pressure-Gradient Correlations in a FORANS Approach to Turbulence Modeling", *AIAA2014-2207*. Atlanta, GA.
- Poroseva, S. V., and Murman S. M., 2014b, "On Modelling Velocity/Pressure-Gradient Correlations in Higher-Order RANS Statistical Closures," *Proc. 19<sup>th</sup> AFMC*, Melbourne, Australia.
- Poroseva, S. V., Colmenares, J. D., Murman S. M., 2015, "RANS Simulations of a Channel Flow with a New Velocity/Pressure-Gradient Model", *AIAA2015-3067*, Dallas, TX.
- Poroseva, S. V., Colmenares, J. D., Murman S. M., 2016a, "On the accuracy of RANS simulations with DNS data", *Physics of Fluids*. Vol. 28(11), DOI: 10.1063/1.4966639
- Poroseva S. V., Jeyapaul, E., Murman S. M., Colmenares, J. D., 2016b, "The Effect of the DNS Data Averaging Time on the Accuracy of RANS-DNS Simulations", *AIAA2016-3940*, Proc. AIAA Aviation, Washington DC June 13-17, 2016.

Sillero J. A., Jiménez, J., Moser, R. D., 2013, "One-Point Statistics for Turbulent Wall-Bounded Flows at Reynolds Numbers up to  $\delta^+ = 2000$ ", *Phys. Fluids*, Vol 25(10), pp. 1-15.

Spalart P. R., 1988, "Direct simulation of a turbulent boundary layer up to  $Re_\theta = 1410$ ", *J. Fluid Mech.*, Vol. 187, pp. 61-98.

FIGURE

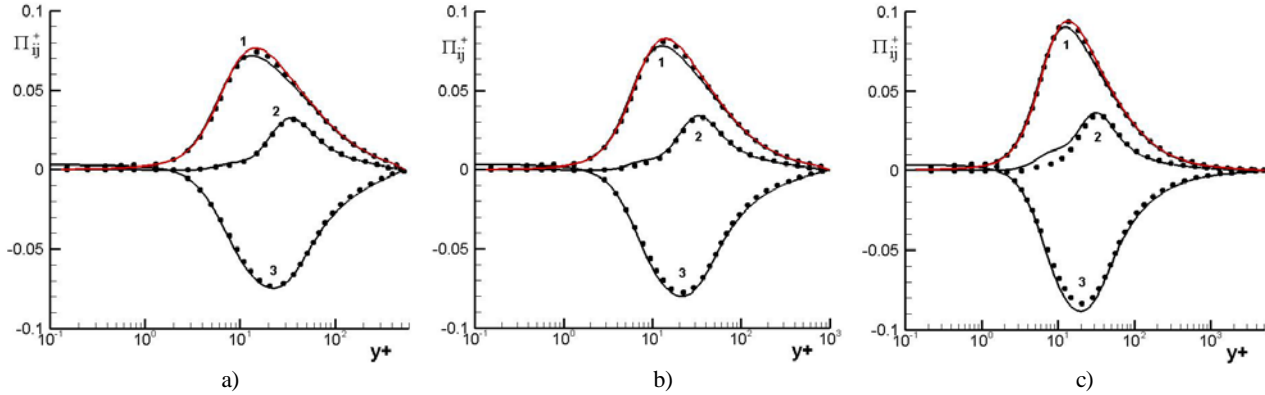


Figure 1. Validation of models (1) in a fully developed channel flow with DNS data from Lee and Moser (2015) at  $Re_\tau$  a) 550, b) 1000, and c) 5200. Notations: solid lines are profiles of the VPG correlations calculated from (1), symbols are the DNS data. Line labels: 1 –  $\Pi_{xy}$ , 2 –  $\Pi_{yy}$ , and 3 –  $\Pi_{xx}$ .

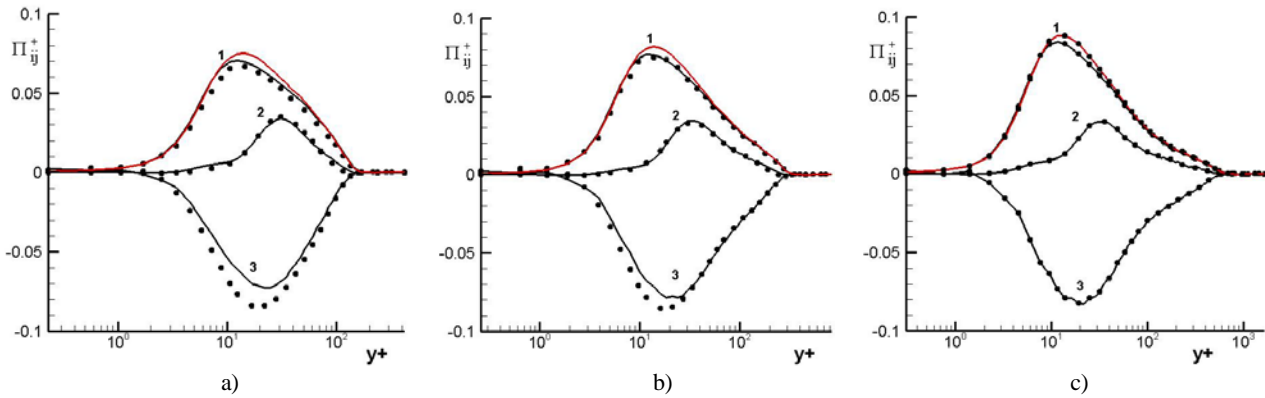


Figure 2. Validation of model expressions (1) in a ZPGBL with DNS data from Spalart (1988) at  $Re_\theta$  a) 300, b) 670, and c) 1410. Notations are as in Fig. 1.

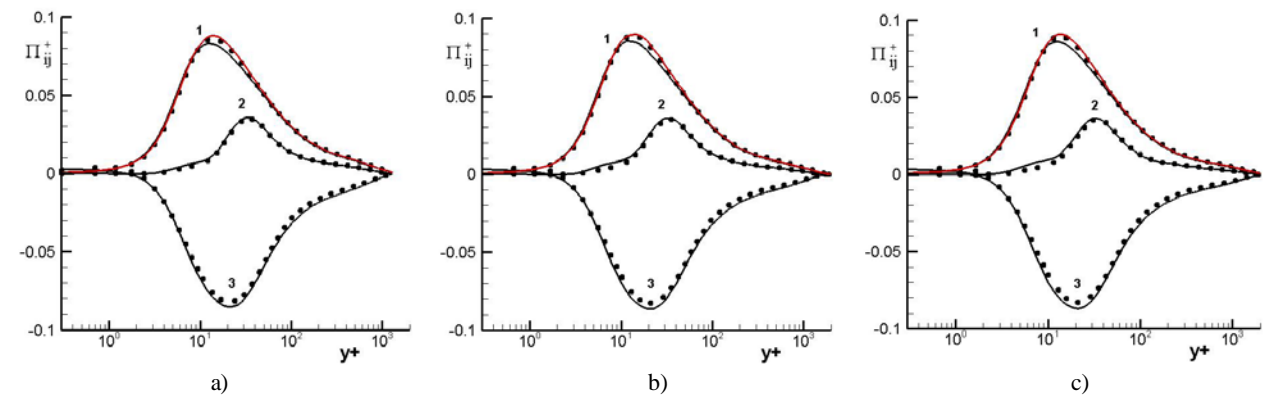


Figure 3. Validation of model expressions (1) in a ZPGBL with DNS data from Sillero et al. (2013) at  $Re_\theta$  a) 4000, b) 5500, and c) 6500. Notations are as in Fig. 1.

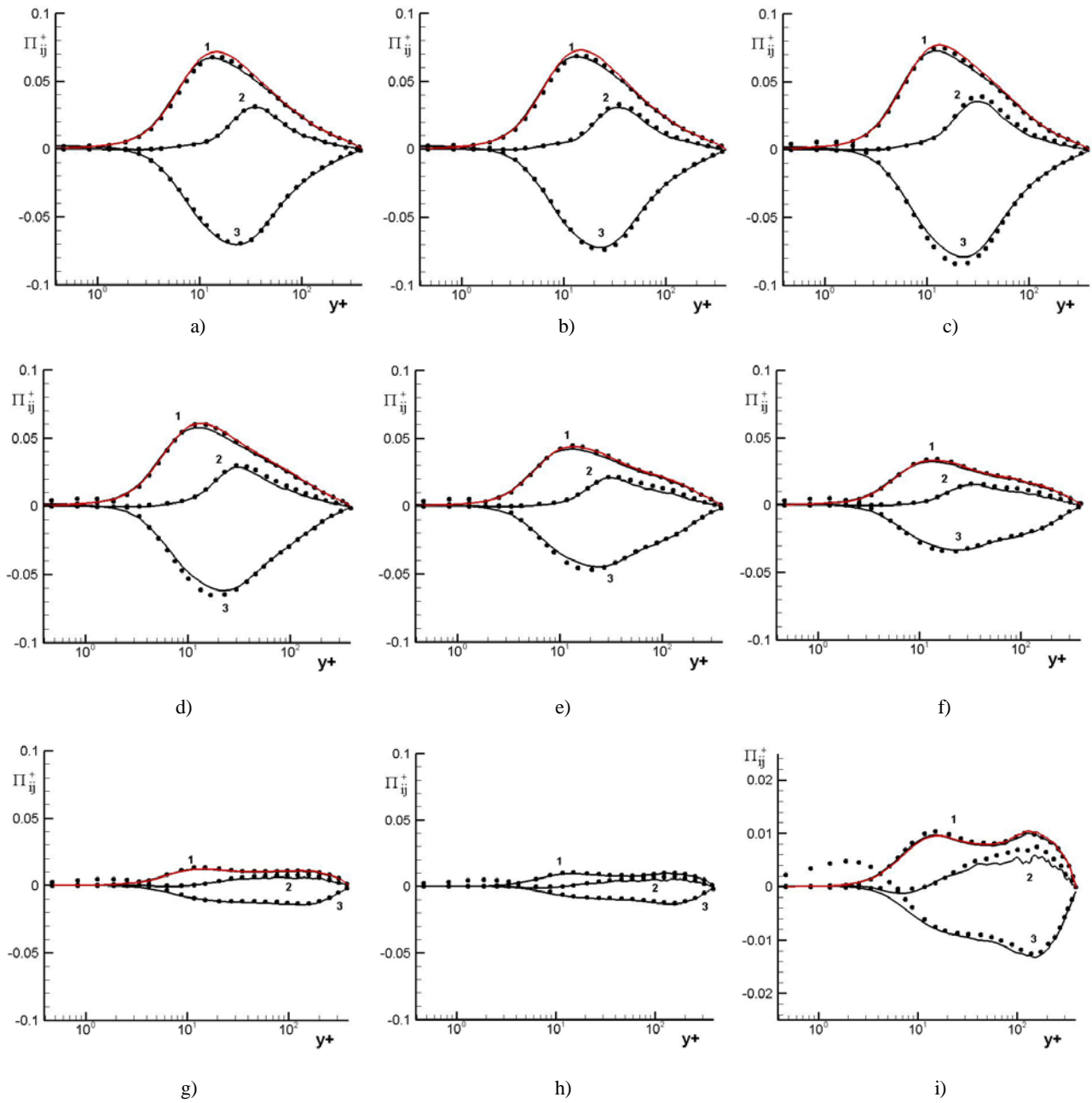


Figure 4. Validation of model expressions (1) in a strained channel flow with DNS data from Coleman et al. (2003) at  $Re_\tau = 392$  and  $A_{22}t$  equal to a) 0, b) 0.02, c) 0.1, d) 0.191, e) 0.281, f) 0.365, g) 0.675, h,i) 0.772. Notations are as in Fig. 1, red lines are solutions of (4). The figures h) and i) are the same, but with the different vertical axis scales.

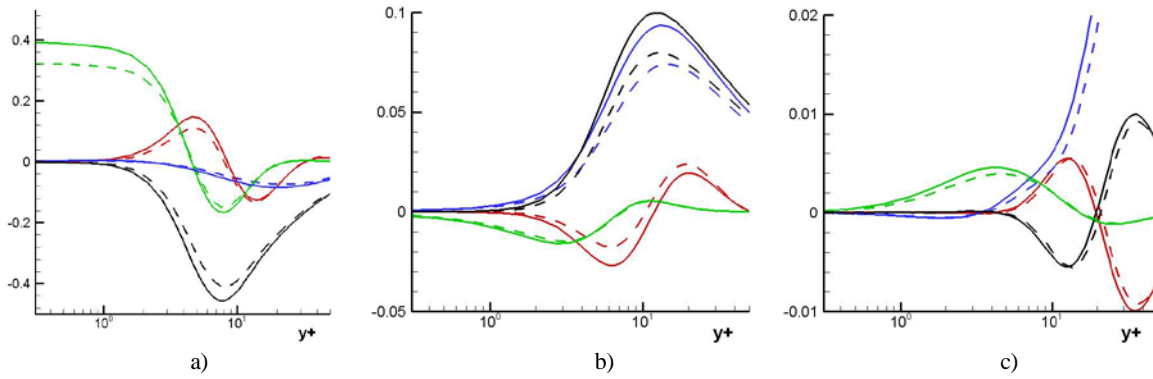


Figure 5. Terms in the transport equations of a)  $\langle u^2 \rangle$ , b)  $\langle uv \rangle$ , and c)  $\langle v^2 \rangle$  from DNS of Lee & Moser (2015) in the near-wall flow area. Notations: —  $Re_\tau = 5200$  and --  $Re_\tau = 550$ . Color scheme: blue  $\Pi_{ij}$ , green  $D_{ij}^M$ , red  $D_{ij}^T$ , black  $D_{ij}^M + \Pi_{ij} - \varepsilon_{ij} - Err_{ij}$ .

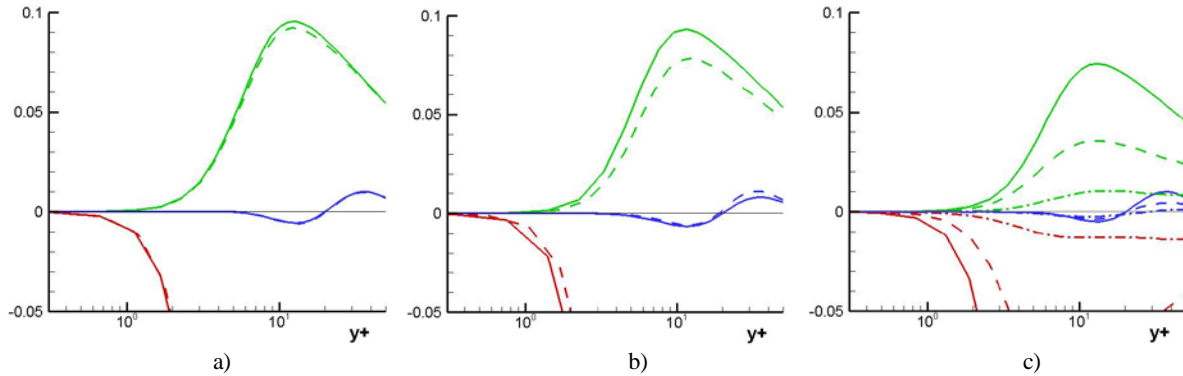


Figure 6. Profiles of  $D_{ij}^M + \Pi_{ij} - \varepsilon_{ij} - Err_{ij}$  obtained with DNS data from of a) Sillero et al. (2013), b) Spalart (1981), and c) Coleman et al. (2003) in the near-wall flow area. Notations: a) —  $Re_\theta = 6500$  and --  $Re_\theta = 4000$ ; b) —  $Re_\theta = 1410$  and --  $Re_\theta = 300$ ; c) —  $A_{22}t = 0$ , --  $A_{22}t = 0.365$ , and - · -  $A_{22}t = 0.772$ . Color scheme: green for  $\langle uv \rangle$ , blue for  $\langle v^2 \rangle$ , and red for  $\langle u^2 \rangle$  budgets.

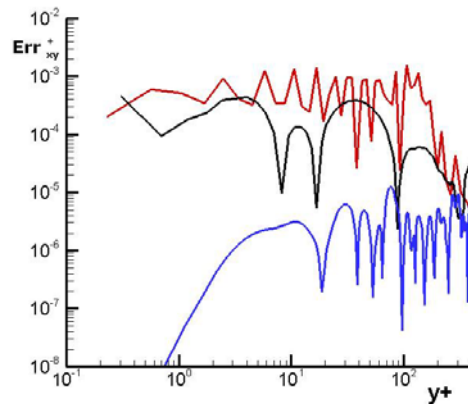


Figure 7. Profiles of the balance errors in the  $\langle uv \rangle$ -budgets of DNS data: — Spalart (1981) at  $Re_\theta = 300$ , — Lee and Moser (2015) at  $Re_\tau = 5200$ , and — Sillero et al. (2013) at  $Re_\theta = 4000$ .